Uniaxial Compression of Porous Magnetorheological Elastomer

Mohammad Yousef Amer Hdaib[1,a] and Iva Petríková[1,b]

[1]*Technical University of Liberec; Studentská 1402/2, Liberec, Czech Republic;*

[a]*mohammad.yousef.hdaib@tul.cz*, [b]*iva.petrikova@tul.cz*

Abstract: The development and progression of robotics and sensors expand the requirements for intelligent materials. Thus, this study is concerned with the fabrication, material modeling, and experimentation of Magnetorheological elastomer in foam structure (MREF). The MREF comprised a synthetic silicon matrix filled with iron particles. The magnetoelastic and hyperelastic parameters were identified using a modified compressible Mooney-Rivlin model. The engineering stress was derived based on decomposing the constitutive relation into isochoric and volumetric parts. Then the material parameters were identified for uniaxial compression of MREF in the presence and absence of a magnetic field. The model fitted the experimental data accurately with similar behavior reported in the literature.

Keywords: MRE; Porous magnetorheological elastomer; Magneto-hyperelastic model; Highly-compressive MRE.

1 Introduction

The fabricated Magnetorheological elastomeric foam (MREF) consists of a porous rubber matrix filled with carbonyl iron particles. Such Magnetoelastic material has adjustable stiffness with a magnetic field and vice versa. Particularly, the MREF exhibits a noticeable change in magnetization with displacement because it is highly compressive, which makes it suitable for soft robotics like tactile sensors [1].

To estimate the magnetoelastic coupling for MREF and to employ it for finite element analysis, it is crucial to derive a suitable compressive form of engineering stress. For conventional magnetorheological elastomer (MRE), Kankanala et al. [2,3] derived the constitutive relations for the Cauchy stress, magnetic field, and entropy. The authors derived identical constitutive relations based on Eulerian and Lagrangian forms. In addition, they illustrated how magnetization, magnetostriction, and stress behave with displacement and magnetic field. Afterward, Dorfmann and Ogden [4] proposed a more simplified form of the constitutive relations by merging the magnetic body stresses with the Cauchy stress into a total stress tensor ($\boldsymbol{\tau}$). Subsequently, based on the Dorfmann and Ogden derivation of the total stress tensor, Ottenio et al. [5] illustrated the incremental formulation of magnetoelastic coupling and proposed a modified Mooney-Rivlin Hyperelastic model. The proposed model proved numerical stability through literature based on the results acquired by Marvalova et al. [6] and Janbaz et al. [7].

In this study, an isotropic MREF sample was fabricated using a soluble mold, synthetic silicon rubber, and iron particles. The engineering stress for a highly compressive MREF was derived based on the decomposition of the stress tensor into isochoric and volumetric terms [8]. In addition, the derived form of engineering stress was compared with experimental data.

2 Theory

Eq. (1) and Eq. (2) illustrates the constitutive relation for the total stress ($\boldsymbol{\tau}$) and magnetic field ($\mathbf{H}$), respectively. This formation is derived based on the total stress proposed by

Dorfmann and Ogden [4] and its decomposition into isochoric and volumetric parts, as illustrated by Holzapfel [8].

$$\boldsymbol{\tau} = \boldsymbol{\tau}_{\mathbf{vol}} + \boldsymbol{\tau}_{\mathbf{iso}} \tag{1}$$

$$\boldsymbol{\tau} = \frac{\partial \psi_{\mathbf{vol}}(J)}{\partial J}\mathbf{I} + 2J^{-1}\mathbf{F}.\frac{\partial \psi_{\mathbf{iso}}(\bar{\mathbf{C}},\mathbf{B_L})}{\partial \mathbf{C}}.\mathbf{F}^{\mathbf{T}} \tag{2}$$

$$\mathbf{H} = J^{-1}\frac{\partial \psi(\mathbf{C},\mathbf{B_L})}{\partial \mathbf{B}} \tag{3}$$

The partial differentiation in Eq. (2) and (3) can be expanded additively as:

$$\frac{\partial \psi}{\partial \mathbf{C}} = \sum_{i=1}^{6}\frac{\partial \psi}{\partial \mathbf{C}}\frac{\partial \mathbf{C}}{\partial \mathbf{I}_i} \tag{4}$$

$$\frac{\partial \psi}{\partial \mathbf{B}} = \sum_{i=1}^{6}\frac{\partial \psi}{\partial \mathbf{B}}\frac{\partial \mathbf{B}}{\partial \mathbf{I}_i} \tag{5}$$

Considering a quasi-static case and isotropic material, the total stress and magnetic field take the following tensorial forms:

$$\boldsymbol{\tau} = \frac{\partial \psi_{\mathbf{vol}}(J)}{\partial J}\mathbf{I} + 4J^{-1}\left[J^{-2/3}\frac{\partial \psi_{\mathbf{iso}}}{\partial \mathrm{I}_1}\mathbf{C} + J^{-4/3}\frac{\partial \psi_{\mathbf{iso}}}{\partial \mathrm{I}_2}(\mathrm{I}_1\mathbf{C} - \mathbf{C}.\mathbf{C}) + \frac{\partial \psi_{\mathbf{iso}}}{\partial \mathrm{I}_5}\mathbf{B}\mathbf{B}\right] \tag{6}$$

$$\mathbf{H} = 2\left(\frac{\partial \psi_{\mathbf{iso}}}{\partial \mathrm{I}_4}\mathbf{C}^{-1}.\mathbf{B} + \frac{\partial \psi_{\mathbf{iso}}}{\partial \mathrm{I}_5}\mathbf{B}\right) \tag{7}$$

The used energy function was proposed by Ottenio et al. [5] as follows:

$$\psi_{\mathrm{iso}}(\mathbf{F},\mathbf{B_L}) = C_{10}(\bar{I}_1 - 3) + C_{01}(\bar{I}_2 - 3) + \frac{1}{\mu_0}(\alpha I_4 + \beta I_5) \tag{8}$$

$$\psi_{\mathrm{vol}}(J) = \frac{1}{2}\kappa(J-1)^2 \tag{9}$$

The engineering stress and magnetic field are derived by expanding Eq. (6) and (7) for the principal directions with the following considerations: uniaxial boundary conditions $\left(\lambda_1 = \lambda,\ \lambda_2 = \lambda_3 = \sqrt{J/\lambda}\right)$, magnetic field parallel with the loading direction ($\mathrm{B}_1 = \mathrm{B},\ \mathrm{B}_2 = \mathrm{B}_3 = 0$), and engineering (nominal) stress ($\mathbf{T} = J\mathbf{F}^{-1}\boldsymbol{\tau}$). Eq. (10) and (11) illustrate the derived engineering stress and magnetic field, respectively.

$$\mathrm{T}_{\mathrm{eng}} = \mathrm{C}_{10}\left(\lambda - \frac{J}{\lambda^2}\right)J^{-2/3} + \mathrm{C}_{01}\left(1 - \frac{J}{\lambda^3}\right)J^{-1/3} + \beta\frac{\mathrm{B}^2}{\lambda\mu_0} \tag{10}$$

$$\mathrm{H} = \frac{2\mathrm{B}}{\mu_0}\left(\frac{\alpha}{\lambda} - \beta\lambda\right) \tag{11}$$

3 Experimental measurements

The foam MRE sample was fabricated using liquid silicon rubber, iron particles, 3d-printed mold, and soluble mold (sugar) according to the following steps:

- The following raw materials were mixed: silicone, hardener, and iron particles.
- The mixture was vacuumed and poured on the soluble mold (rigid sugar) inside the 3d-printed assembly, as shown in Fig. 1b and c.
- The whole mixture with sugar was left for setting in the fridge for 72 hours. In this context, setting means providing enough time for the mixture to flow inside the small canals between the sugar crystals.
- The mixture was left to polymerize in a vacuum at room temperature.
- The sugar-MRE texture was cut off from the polymerized mixture, as shown in Fig. 1d.
- The sugar-MRE texture was sunk in water for 24 hours, at which the sugar melted, and the MREF sample was acquired. The sample porosity (ϕ) was calculated using the occupied volume by MRE ($\mathrm{V}_{\mathrm{MRE}}$), as follows:

$$\phi = 1 - \frac{V_{MRE}}{V_{total}} \tag{12}$$

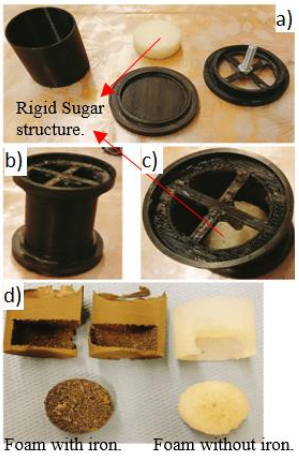

Fig. 1. Sample fabrication.

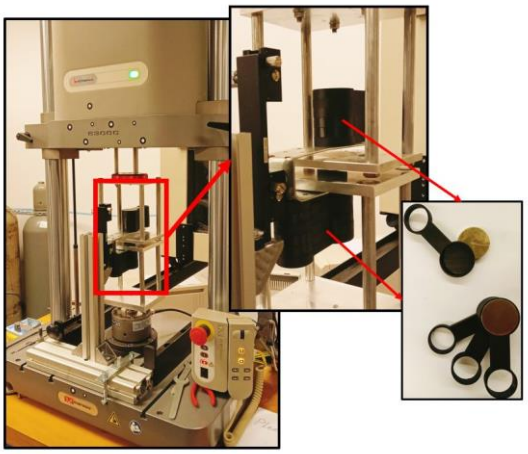

Fig. 2. Experimental setup.

The uniaxial compression was performed using Instron E3000 with grips designed to attach neodymium magnets and prevent them from interfering with the signal of the displacement sensor. The grips are made from Aluminum and brass to avoid interference with the magnetic field. As shown in Fig. 2, the magnetic field can be adjusted by changing the number of magnets.

4 Results

Fig. 3 illustrates a quasi-static uniaxial compression with a 0.003 s^{-1} strain rate. The sample was compressed to a 0.7 stretch (λ) at variable magnetic fields. The dotted curves represent the experimental data, while the solid ones represent the theoretical model (Eq. 10).

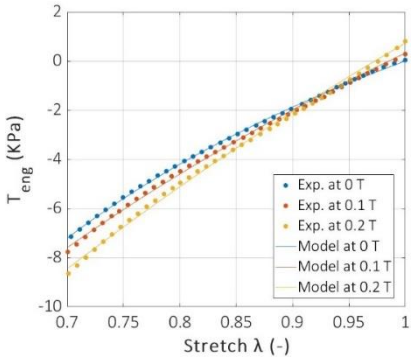

Fig. 3. Theoretical model fitting results with a quasi-static uniaxial compression for MRE foam.

Table 1. Material parameters.

	At 0 [T]	**At 0.1 [T]**	**At 0.2 [T]**
C_{01}[Pa]	-847.11	-4853.2	-7314.9
C_{10}[Pa]	7822.7	13914	18511
α [-]	0	0.387	0.399
β [-]	0	0.0406	0.0229

At zero displacements, a positive stress appears, which agrees with the isotropic MRE behavior reported by Kankanala et al. [2]. Moreover, the engineering stress increases with the magnetic field, and the maximum magnetorheological effect equals 8.7% and 20% at 0.1 T and 0.2 T, respectively. For the fitting model, a Poisson ratio of 0.22 was used based on a study performed by Sanborn et al. [9]. The theoretical model predicted the material behavior accurately using parameters shown in Table 1.

Conclusion

In this study, an isotropic MRE foam sample was fabricated using a soluble mold, liquid silicon, and carbonyl iron particles. The engineering stress was derived for compressible MREF. The magneto-hyperelastic parameters were identified using data from uniaxial compression in the presence and absence of a magnetic field.

For the fabrication process, the authors recommend using a less viscous liquid silicon rubber to reduce the setting time and acquire stiffer samples. In contrast, the theoretical model can be improved by including the porosity in the volumetric part of the energy function, which simultaneously treats the fabricated sample as porous and compressible.

Acknowledgment

This publication was written at the Technical University of Liberec as part of the project "Research of advanced materials, and application of machine learning in the area of control and modeling of mechanical systems" nr. SGS-2022-5072 with the support of the Specific University Research Grant, as provided by the Ministry of Education, Youth and Sports of the Czech Republic in the year 2022.

References

[1] Diguet, G., Froemel, J., Muroyama, M. and Ohtaka, K. "Tactile Sensing Using Magnetic Foam," *Polymers*, **14**(4), 834 (2022).

[2] Kankanala, S.V. and Triantafyllidis, N. "On finitely strained magnetorheological elastomers," *J Mech Phys Solids*, **52**(12), pp. 2869-2908 (2004).

[3] Danas, K., Kankanala, S.V. and Triantafyllidis, N. "Experiments and modeling of iron-particle-filled magnetorheological elastomers," *J Mech Phys Solids*, **60**(1), pp. 120-138 (2012).

[4] Dorfmann, A. and Ogden, R.W. "Nonlinear magnetoelastic deformations of elastomers," *Acta Mech*, **167**(1–2), pp. 13-28 (2004).

[5] Otténio, M., Destrade, M. and Ogden, R.W. "Incremental magnetoelastic deformations, with application to surface instability," *J Elast*, **90**(1), pp. 19-42 (2008).

[6] Marvalová, B. and Petríková, I. "Modelling of magneto-mechanical coupling in COMSOL multiphysics," in *Const Models for Rubber IX*, Marvalová B. and Petríková I. ed. (CRC Press, London, 2015), pp. 657–662.

[7] Janbaz, M. and Saeidi Googarchin, H. "Experimental and numerical analysis on magneto-hyper-viscoelastic constitutive responses of magnetorheological elastomers: A characterization procedure," *Mech Mater*, **154**, 103712 (2021).

[8] Holzapfel, G. "Nonlinear Solid Mechanics: A Continuum Approach for Engineering Science," *Meccanica*, **37**(4–5), pp. 489-490 (2002).

[9] Sanborn, B. and Song, B. "Poisson's ratio of a hyperelastic foam under quasi-static and dynamic loading," *Int J Impact Eng*, **123**(1), pp. 48-55 (2019).